This is the Pre-Published Version.

The following publication Yang, D., Zhang, L., Luo, M., & Li, F. (2020). Does shipping market affect international iron ore trade?– An equilibrium analysis. Transportation Research Part E: Logistics and Transportation Review, 144, 102107 is available at https://dx.doi.org/10.1016/j.tre.2020.102107.

Does shipping affect the international iron ore trade? – An equilibrium analysis

Abstract

The impacts of shipping on the iron ore trade has become a hot topic in the industry over recent years. To evaluate such impacts, a mixed complementarity-based equilibrium model is built to capture the strategic behavior and interaction among the major players in the market, including importers, exporters, and carriers. In this three-party equilibrium model, importers and exporters compete in a Cournot fashion incorporating the shipping cost, which is endogenized by a transportation optimization problem. This model is an instance of the Discretely Constrained Mixed Complementarity Problem (DC-MCP), and a solution procedure for this problem is provided based on a Mixed Integer Nonlinear Program (MINLP) reformulation and convexification techniques. The model has real data applied to it so as to evaluate the impact on its iron ore trade volume of large-size ship adoption in Brazilian iron ore exports. The results show that increasing the number of large ships leads to a decrease in freight rate, adjustment of export capacity restrictions, and increase in fleet capacity. These three factors jointly drive the trade volume up, whereas their impacts are different.

Key words: *Iron ore trade, Bulk Shipping, Large ships, Three-party equilibrium, Mixed complementarity problem*

1. Introduction

In the international iron ore market, Asian countries, especially China, Korea, and Japan, are the major importers, accounting for 85.7% of global iron ore imports in 2016, while Australia and Brazil are the two major exporters, having enjoyed 77.33% market share of global iron ore exports in 2016 (World Steel Association Report, 2018). Due to its closer transport distance to Asia, Australia dominates the Asian iron ore imports, accounting for 63.12% of the market share in 2016 (World Steel Association Report, 2018). Being located far away from its major importers, Brazil has competed with Australia for the Asian market by initiating a series of shipping strategies. For example, Brazil miners (the Valley, Companhia Siderrgica Nacional) have deployed very large bulk ships (400,000 tonnes Valemax) for their iron ore transportation, cooperating since 2012 with giant Chinese carriers, such as China Merchants Group and China Ocean Shipping Company. At the same time, these Brazil miners have also built self-owned specialized terminals for iron ore handling in order to increase their iron ore sea handling capacity and reduce their shipping costs in the East Asia trade. However, these strategies seem to be ineffective. As an evidence, from 2012 to 2015, the iron ore exported from Brazil to East Asian countries grew by only 10.2%, while Australian

© 2020. This manuscript version is made available under the CC-BY-NC-ND 4.0 license http://creativecommons.org/licenses/by-nc-nd/4.0/.

exports increased by 54.6%. This raises doubts as to whether it is worthwhile for Brazil miners to put so many efforts into improving the sea transportation of iron ore. In this study, we develop an analytical tool to evaluate the impact of shipping on the international iron ore trade.

The computable equilibrium model is one of the most widely applied approaches to both strategy and policy analysis in the international resource commodity markets. Based on the assumption of market structure and individual behavior, the optimization problems of major players and market clearing conditions are formulated into an equilibrium framework to simulate the interrelations of the players in an economic system. Compared to the analysis of other major resource commodities, e.g., LNG and electricity, equilibrium analysis of the iron ore market attracts only limited attention. Some existing studies have employed the Computable General Equilibrium (CGE) models (e.g., Wang et al., 2007; Ye, 2008) to analyze the responses of leading macroeconomic indices (e.g., GDP and overall trade volume) to the price changes of the iron ore trade. These models focus on the input-output relationships among sectors of an economy system, but ignore many of the industrial features, e.g., the oligopolistic market structure, the restrictions of production capacity, diversified trade costs, etc., which are critical factors in the iron ore trade.

In the existing equilibrium studies of international resource trade, shipping demand is broadly regarded as a derived demand, with the impact of shipping sectors not generally being considered in the trade analysis. As a matter of fact, it is generally believed that trade volume is not that much related to the freight rate. However, recently some researchers have presented evidence suggesting that the importance of the freight rate in the international resource trade cannot be ignored. For example, Bai and Lam (2019) applied a structural equation model to analyze the various relationships between fleet size, trade demand, freight rates, and ship prices in a very large gas carrier market. They found that the Liquefied Petroleum Gas trade is highly correlated to the change of freight rate. Li et al. (2019) proved that the fleet deployment has an impact on the iron ore international trade volume to China, through building a ship scheduling optimization model. It is noticed that these studies focus only on the transportation sector but ignore the interactions with other trade sectors.

To fill this research gap, in this study we propose a general iron ore trade equilibrium model by: i) developing a supply/demand model for the trade between exporters and importers, which allows for the analysis of an oligopolistic market structure and the endogenous export capacities of exporters; ii) endogenizing the iron ore shipping cost through a transportation optimization model, which enables the evaluation of the impact of shipping on the iron ore trade.

Due to the existence of integer variables (e.g., ship number), this model is formulated as a Discretely Constrained Mixed Complementarity Problem (DC-MCP), which is difficult to be solved. In this paper, we therefore design a solution procedure for it. In particular, we look for the

near complementarity solutions of the model by applying a mixed integer nonlinear programming (MINLP) formulation and convexification techniques. A case study with real data is conducted to validate both the model and the proposed procedure.

The contributions of this study are three-fold. First, we investigate the impact of shipping on the international iron ore trade, which is a hot issue in the industry and will be of significance to the future strategy development of shipping carriers and miners. Second, we contribute to the application of an equilibrium model in the resource trade literature, through developing a new model framework in the iron ore trade that incorporates a transportation optimization model within it. This model can be adapted for various impact analyses within the international iron ore trade. Third, we collect a massive amount of data and examine a real problem using this model. We find that the freight rate only a minor impact on the trade, but that the impact of fleet capacity is significant.

The rest of the paper is organized as follows: In section 2, we summarize the existing literature with regard to resource commodity market analysis and computable equilibrium models. Section 3 develops a mixed complementarity-based equilibrium model for the proposed international iron ore market. Section 4 provides the solution method for the proposed model. In section 5, we validate our model with real data through analyzing the impact of large ship adoption on the international iron ore trade. Finally, in section 6, we state our conclusions.

2. Literature review

With the development of optimization algorithms and data availability in recent decades, computable equilibrium models have been increasingly applied to the analysis of international resource commodity markets. In particular, due to rapid growth of the natural gas and electricity trades, many computable equilibrium models have been established to evaluate the impact from market structure transition and construction of new infrastructures on price and trade volume in these two markets. The early work on equilibrium models stemmed from the studies on market power and competition patterns in the European natural gas market. Notable examples include GASTALE-Gas mArket System for Trade Analysis in a Liberalizing Europe (Boots et al., 2004), and NATGAS-NATural GAS model (Zwart and Mulder, 2006). GASTALE explores the effect of producers strategic behaviors on gas price and trade volume. NATGAS focuses on the impact from the market structure (i.e., consumer surplus) through deriving more plausible demand functions for gas consumption. As for the North American gas market, Gabriel et al. (2005a) discussed the regional price differentials in the US market through building a large-scale linear complementarity gas equilibrium model. Gabriel et al. (2005b) further presented a general model for the natural gas market, and provided sufficient details to show that the model is an instance of the mixed nonlinear complementarity problem (NCP). This work is a milestone in natural gas market equilibrium

analysis, as it not only provides a standard modeling framework but also proves the existence of equilibrium solutions. Egging et al. (2010) extended the model to the global market and developed the World Gas Equilibrium Model (WGM). In order to be more realistic, WGM updates the market power of gas producers in the upstream market and endogenizes the infrastructure investment. These models have been further extended to study infrastructure constraints (Huppmann, 2013), supply securities in a low-carbon energy system (Holz et al., 2016), impacts of new entrants on market power (Siddiqui et al., 2017), and gas price indexation (Shi and Variam, 2017) etc.

Also, in the electricity market, Green and Newbery (1992) simulated the British electricity market based on a supply function equilibrium of oligopoly structure under uncertainty (Klemperer et al., 1989). Leuthold et al. (2005) built a spatial equilibrium model (ELMOD) for the German electricity market. Weigt et al. (2006) extended the application scope of ELMOD to cover more European regions, including France, Benelux, Western Denmark, Austria and Switzerland. Based on the previous work, Leuthold et al. (2012) made a summary of ELMOD and developed more thorough and specific assumptions so that the large-scale spatial equilibrium model of the European electricity market becomes applicable. As a classical framework, ELMOD has been extended to analyze the impact from the development of transmission facilities between high voltage alternating current and direct current (Egerer et al., 2013), pricing scheme (Neuhoff et al., 2013; Egerer et al., 2016), electricity congestion management (Kunz et al., 2015), renewable energy reform (Janda et al., 2017), political impacts forecasting (Assembayeva et al., 2018), and etc.

It is noted that equilibrium analysis of the natural gas and electricity markets has already achieved many developments and applications. However, the international iron ore market is still an untouched field in which also exists similar structural changes, such as the development of transportation facilities, market restructuring and resource security policy making (Wilson, 2012). As one of a few limited studies in this field, Toweh and Newcomb (1991) presented a spatial equilibrium model to estimate the competitive prices and efficient trade flows in the iron ore trade through a consideration of ex-post-computed transport costs. Wang et al. (2007) applied a CGE model to analyze the impact of world iron ore price fluctuation on the Chinese economy from both macroeconomic indices (e.g., GDP and the price of GDP) and industrial differentiation. Ye (2008) applied a multi-sector dynamic CGE model to estimate the impacts of iron ore boom on national economy performance.

The above models are macro economy-based, and are not applicable to solve our problem for the following reasons. First, they assume that the market is perfectly competitive based on general equilibrium theory, which is not consistent with reality. Germeshausen et al. (2018) suggested the existence of imperfect competition among iron ore producers. Second, using these models, it is hard to solve industrial-economy issues, such as the impact of capacity change of the industrial

sector on the commodity trade, since they ignore the restrictions on the movement of productive endowments and commodities. Third, the shipping cost is treated as one part of the exogenous trade costs, which makes it impossible to explicitly evaluate the complex interaction between the shipping sector and the international iron ore trade. The shipping sector plays an important role in international iron ore trade. For example, Li et al. (2019) found that, when the market chartering price of a large size ship remains high, building a very large ship can be an effective strategy to lower the Brazil iron ore price. However, this impact has never been discussed in an equilibrium modeling framework considering the strategies of various players in this industry. As mentioned by Robson et al. (2018), a computable equilibrium model will help to open the black box where the market mechanics are hidden.

This study will enrich the previous literature on computable equilibrium models by 1) extending its application to the international iron ore market, 2) breaking through the limitation imposed by the perfect competition assumption, and 3) treating the shipping sector as one independent module, which will enable an investigation into the interactions between the iron ore trade and the shipping market.

3. Equilibrium model for iron ore trade market

This section describes a multi-sector mixed complementarity-based equilibrium model. Three major players in the iron ore trade, namely exporters, importers and carriers are considered, each with one module. Importer module and exporter module determine the equilibrium trade volumes and prices though a Cournot competition of exporters incorporating a CES-based inverse demand function. The carrier module endogenizes the shipping sector by assuming perfect competition among carriers in different market segments. Transport flows and fleet deployment in the market segments are determined through a transportation optimization model of the shipping sector. We also introduce a port selection problem to transform the trade volumes into cargo handling volumes at port, which helps in determining the transport volumes in the transportation optimization model. Market clearing and consistency conditions are also presented to connect the different modules and to ensure the equilibrium of the model.

To start, an overview of these players is provided, followed by the definition of notations and finally the description of the model by modules.

3.1. Overview of international iron ore trade players

In general, three major players can be recognized in the international iron ore market, these being importers, exporters and carriers.

- Importers – who have a demand for iron ore and purchase it from various exporters. In this study, importers indicate the iron ore importing countries. We assume that importers are price takers.

- Exporters – who own iron ore resources and produce and export iron ore to various importers. In this study, exporters are the iron ore exporting countries.
- Iron ore carriers – who provide transportation services in the iron ore shipping market. It is generally accepted that the dry bulk shipping market is perfect-competitive (Peng, 2016), in which numerous carriers provide homogenous services, and that it is hardly possible for an individual carrier to own market power. Thus, in this study, we assume that each ship is an independent carrier.

It should be noticed that the port operator is also one of the players, as it provides cargo handling services for the importers/exporters, and ship berthing services for the carriers. Unlike the above three players, who are independent decision makers in this model, we implicitly model the port in the cost function of importers, exporters and carriers.

3.2. Notations

In this section, we discuss the sets of subscripts referring to variables in the model. Importer is denoted by $c \in C$, with C being the set of importers. Exporter is indexed by $m \in M$, with M being the set of exporters. In addition, destination port is denoted by $d \in D(c)$, with $D(c)$ being the set of destination port of importer $c \in C$. The origin port is indicated by $o \in O(m)$ with $O(m)$ being the set of origin ports of exporter $m \in M$. As each ship is an independent carrier in the shipping market, we can classify the carriers in term of ship sizes. For a certain carrier type (carriers with same ship size), we indicate it by $k \in K$, with K being the set of carriers.

Table 1-3 shows the relevant variables of the importer and exporter, the carrier, and the destination/origin port respectively. Table 4 gives the parameters. In this study, we clarify that a bar on a variable x ($\overline{x}$) indicates that the variable is exogenous.

Table 1 Variables of importer and exporter

Variable	*Description*
U_c	Utility of importer c while trading with different exporters.
DC_c	Overall iron ore import volume of importer c ($DC_c > 0$).
I_c	Purchasing budget of importer c.
π_{mc}	Profits of exporter m earned by exporting iron ore to importer c.
QM_m	Overall export volume of exporter m ($QM_m > 0$).
QTC_m	Iron ore production capacity of exporter m.
Q_{mc}	Trade volume between exporter m and importer c ($Q_{mc} > 0$).
P_{mc}	Import price for iron ores from exporter m to importer c ($P_{mc} > 0$).

Table 2 Variables of Carrier

Variable	*Description*
SC	Overall shipping cost in the international iron ore trade.
$QS_{m_o c_d}$	Iron ore shipment volume from origin port o of exporter m to destination port d of importer c.
$N_{km_o c_d}$	Number of k-type ships sailing from origin port o of exporter m to destination port d of importer c ($N_{km_o c_d} \geq 0$).
$F_{km_o c_d}$	Freight rate of k-type ships on the route between port o of exporter m and port d of importer c.
NC_k	Overall number of k-type ships.
W_k	Average deadweight of k-type ships.
OD_k	Annual operating time of k-type ships.
V_k	Average speed of k-type ships.
$L_{m_o c_d}$	Route distance from port o of exporter m to port d of importer c.
MV_{mc}	Annual average voyages that can be arranged between exporter m and importer c.

Table 3 Variables of destination/origin port

Variable	*Description*
CHC_c	Overall cargo handling charges that importer c pays for discharging services provided by all its destination ports.
QD_{c_d}	Discharging volume at destination port d of importer c ($QD_{c_d} > 0$).
PD_{c_d}	Cargo handling price at port d of importer c ($PD_{c_d} > 0$).
DSD_{c_d}	Unit berthing fee at destination port d of importer c.
CHM_m	Overall cargo handling charges that exporter m pays for loading services provided by all origin ports.
QO_{m_o}	Loading volume at origin port o of exporter m ($QO_{m_o} > 0$).
PO_{m_o}	Cargo handling price at port o of exporter m ($PO_{m_o} > 0$).
DSO_{m_o}	Unit berthing fee at origin port o of exporter m.

Table 4 Parameters in the model

Parameter	*Description*
δ^d_{mc}	Share parameter used to determine the share of trade volumes from exporter m to importer c. $\delta^d_{mc} \in (0,1)$, $\sum_{m\in M} \delta^d_{mc} = 1$.
σc_c	Parameter of substitution elasticity among trade volumes trading from exporters to importer c. $\sigma c_c = 1 - \frac{1}{ec_c}$, where $ec_c (ec_c > 1)$ is substitution elasticity.
AC_m	Efficiency parameter in CET function.
δ^s_{mc}	Share parameter used to determine the share of export capacities from exporter m to importer c. $\delta^s_{mc} \in (0,1)$, $\sum_{c\in C} \delta^s_{mc} = 1$.
σm_m	Parameter of transformation elasticity among export capacities allocated by exporter m to importers. $\sigma m_m = 1 - \frac{1}{ec_c}$, where $em_m (em_m < 0)$ is transformation elasticity.
AD_c	Efficiency parameter of CES function for destination ports of importer c.
$\delta^{DP}_{c_d}$	Share parameter used to determine the share of imports discharging at port d of importer c. $\delta^{DP}_{c_d} \in (0,1)$, $\sum_{d\in D(c)} \delta^{DP}_{c_d} = 1$.
σd_c	Parameter of substitution elasticity among ports of importer c. $\sigma d_c = 1 - \frac{1}{ed_c}$, where $ed_c (ed_c > 1)$ is substitution elasticity.
AO_m	Efficiency parameter of CES function for origin ports of exporter m.
$\delta^{OP}_{m_o}$	Share parameter used to determine the share of exports loading at port o of exporter m. $\delta^{OP}_{m_o} \in (0,1)$, $\sum_{o\in O(m)} \delta^{OP}_{m_o} = 1$.
σo_m	Parameter of substitution elasticity among ports of exporter m. $\sigma o_m = 1 - \frac{1}{eo_m}$, where $eo_m (eo_m > 1)$ is substitution elasticity.

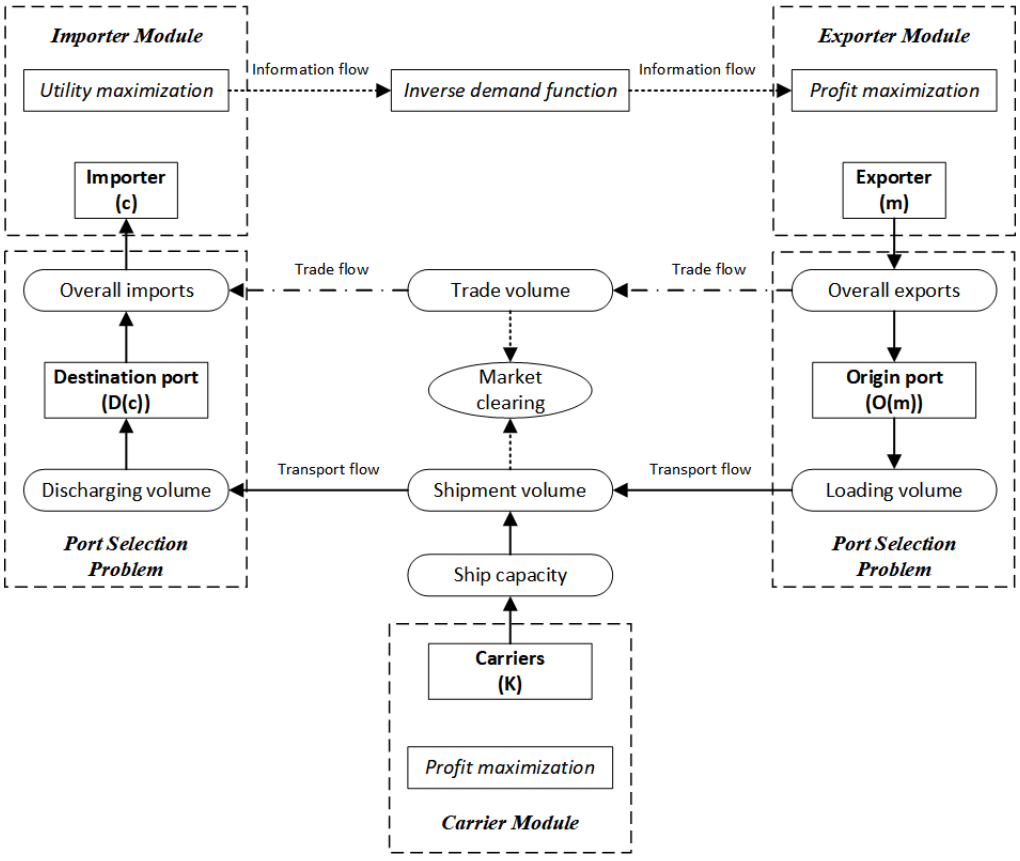

Figure 1 Structure of iron ore equilibrium model

3.3. Module description

Figure 1 shows the structure of our model. Three modules describe the strategies of the importer, exporter and carrier. Importer module represents the utility maximization problem of the importer when importing the iron ore from exporters. With the perfect information, the inverse demand function is available to the exporter. In exporter module, based on the inverse demand function, the exporter maximizes its profit through determining its trade volume. In carrier module, to maximize its profit, the carrier arranges appropriate ship capacities for the shipment volume in transport flow from the origin ports to the destination ports. To determine the shipment volume, its required to know the discharging/loading volume of the port. In the model, we interpose a port selection problem which describes mechanism how the import/export volume are allocated to ports. The inter-sector equilibrium between the trade and shipping sector is ensured by the marketing clearing conditions between the trade volume and the shipment volume. In the following part, we will model the three modules and the allocation problem respectively.

3.3.1. Importer module

The importer module describes the rational behaviors of importers in the international iron ore trade. Each importer has a given purchasing budget for iron ore imports. Since importers are price takers and the iron ores from different exporters are not perfect substitutes, each importer maximizes its utility by choosing appropriate proportions of iron ores from different exporters within the budget constraint. For an importer c, its utility maximization can be described as follows:

$$\max_{Q_{mc}} \quad U_c = (\sum_{m\in M} \delta^d_{mc} Q_{mc})^{\frac{1}{\sigma c_c}}, \tag{1a}$$

$$\text{s.t.} \quad \sum_{m\in M} P_{mc} Q_{mc} = \overline{I_c} \quad (\gamma^U_c) \quad \forall c, \tag{1a.1}$$

where γ^U_c ($\gamma^U_c free$) is the shadow price corresponding to constraint (1a.1). The parameter of elasticity $\sigma c_c (\sigma c_c = 1 - 1/ec_c)$ satisfies $\sigma c_c \in (0,1)$, since $ec_c > 1$.

In order to represent the imperfect substitution relationships among different exporters, a Constant Elasticity of Substitution (CES) utility function is applied to represent the consumption utility maximization as (1a). Constraint (1a.1) indicates the budget constraint of importer c. Because the utility function satisfies the strict convex preference, we can derive a unique inverse demand function ($P_{mc}(\cdot)$) to describe the relationship between trade price and volume based on the corresponding First Order Conditions (FOCs). Therefore, for a given trade between exporter m and importer c, the inverse demand function can be shown as the equation (1b).

$$P_{mc} = P_{mc}(Q_{mc}, Q_{m'c}) = \frac{\overline{I_c} \delta^d_{mc} {Q_{mc}}^{(\sigma c_c - 1)}}{\delta^d_{mc} {Q_{mc}}^{\sigma c_c} + \sum_{m'\in M\setminus m} \delta^d_{m'c} {Q_{m'c}}^{\sigma c_c}} \quad \forall m, c, \tag{1b}$$

where $\sigma c_c = 1 - 1/ec_c$ along with $ec_c > 1$, $\sigma c_c \in (0,1)$, $m' (m' \in M \setminus m)$ is a rival of exporter $m \in M$.

3.3.2. Exporter module

The international iron ore market is widely regarded as an oligopoly market dominated by several major exporters, e.g., Brazil and Australia (e.g., Pustov et al., 2013). They use quantity of output to maximize their own profits, which can be described as:

$$\max_{Q_{mc}} \quad \pi_{mc} = [P_{mc}(Q_{mc}, Q_{m'c}) - PC_c - TC_{mc}]\, Q_{mc}, \tag{2a}$$

$$\text{s.t.} \quad Q_{mc} \le QC_{mc} \quad (\gamma_{mc}^{QC}) \quad \forall m, c, \tag{2a.1}$$

$$\sum_{m\in M}\sum_{c\in C} \frac{Q_{mc}}{\overline{MV}_{mc}} \le \sum_{k\in K} \overline{NC}_k \overline{W}_k \quad (\gamma^{NC}), \tag{2a.2}$$

where PC_c ($PC_c \ge 0$) is the average cargo handling price at the destination ports of importer c, TC_{mc} is the unit trade cost of exporter m in the trade with importer c, QC_{mc} is the endogenous iron ore export capacity of exporter m to importer c ($QC_{mc} \ge 0$), γ_{mc}^{QC} and γ^{NC} ($\gamma_{mc}^{QC}, \gamma^{NC} \ge 0$) are the shadow prices corresponding to constraints (2a.1) and (2a.2).

In the objective function (2a), $P_{mc}(Q_{mc}, Q_{m'c}) - PC_c$ indicates the FOB price offered by exporter m to importer c. TC_{mc} can be further split into following cost items:

$$TC_{mc} = \overline{CQ}_m + F_{mc} + PM_m \quad \forall m, c, \tag{2b}$$

where $\overline{CQ}_m$ is the unit production cost of exporter m, $F_{mc}(F_{mc} \ge 0)$ is the average freight rate from exporter m to importer c, $PM_m(PM_m \ge 0)$ is the average cargo handling price at origin ports of exporter m. Constraint (2a.1) specifies that the trade volumes (Q_{mc}) should be less than the export capacities. Constraint (2a.2) guarantees that the overall fleet capacities can meet the transportation demand of trade.

Since TC_{mc} is linear and $P_{mc}Q_{mc}$ is concave given that $Q_{m'c}$ is fixed and $\sigma c_c \in (0, 1)$, the KKT conditions of (2a) are sufficient for optimality, which can be shown in (2c)-(2e):

$$0 \le Q_{mc} \perp \left[-(P_{mc} - PC_c - TC_{mc}) - \frac{\partial P_{mc}(Q_{mc}, Q_{m'c})}{\partial Q_{mc}} Q_{mc} + \gamma_{mc}^{QC} + \frac{\gamma^{NC}}{\overline{MV}_{mc}} \right] \ge 0 \quad \forall m, c, \tag{2c}$$

$$0 \le \gamma_{mc}^{QC} \perp [QC_{mc} - Q_{mc}] \ge 0 \quad \forall m, c, \tag{2d}$$

$$0 \le \gamma^{NC} \perp \left[\sum_{k\in K} \overline{NC}_k \overline{W}_k - \sum_{m\in M}\sum_{c\in C} \frac{Q_{mc}}{\overline{MV}_{mc}} \right] \ge 0. \tag{2e}$$

Given that the production capacity ($\overline{QTC}_m$) of exporter is exogenous, the export capacity (QC_{mc}) can be regarded as the production capacity allocated to each importer. The relationships between the $\overline{QTC}_m$ and QC_{mc} is subject to the Production Possibility Frontier (PPF), which can be presented through a Constant Elasticity of Transformation (CET) function (Wing, 2004). The exporters need to maximize their trade revenue under zero profit condition ($P_{mc} - PC_c = TC_{mc}$)

under the constraint of PPF. The endogenous export capacity of an exporter m to an importer c then can be derived from the following optimization problem:

$$\max_{QC_{mc}} \quad TRR_m = \sum_{c \in C} TC_{mc} QC_{mc}, \tag{2f}$$

$$\text{s.t.} \quad \overline{QTC}_m = AC_m \left(\sum_{c \in C} \delta_{mc}^s {QC_{mc}}^{\sigma m_m} \right)^{\frac{1}{\sigma m_m}} \quad (\gamma_m^{QTC}) \quad \forall m, \tag{2f.1}$$

where TRR_m denotes the revenue of exporter m, while the FOB price equals to the unit trade cost, $\gamma_m^{QTC}(\gamma_m^{QTC} free)$ is the shadow price corresponding to constraint (2f.1).

Based on FOCs of (2f), the export capacity of exporter m to importer c is given as:

$$QC_{mc} = \frac{\overline{QTC}_m}{AC_m} \left(\frac{\delta_{mc}^s}{TC_{mc}} \right)^{em_m} \left(\sum_{c \in C} {\delta_{mc}^s}^{em_m} {TC_{mc}}^{1-em_m} \right)^{-\frac{1}{\sigma m_m}} \quad \forall m, c. \tag{2g}$$

The iron ore export market is broadly regarded as Cournot competition (Lundmark et al. 2008). However, Hecking and Panke (2015) indicated that the actual market structure is complex with multiple exporters, heterogenous costs, spatial differences with multiple importers and capacity constraints. In order to figure out the exact competitive pattern of the exporters, we apply the conjectural variance approach by conjecturing on the reaction of other rivals when a competitor changes its output or price (Perry, 1982). This makes it available to represent a wide range of market competition structure from Cournot competition to perfect competition (Wogrin et al., 2013). For an exporter m and its rival $m'(m' \in M \setminus m)$ trading with importer c, the conjectural variation of exporter m to rival m' in its trade with importer c is expressed as:

$$\mu_{mm'c} = \frac{\partial Q_{m'c}}{\partial Q_{mc}} \quad \forall m, m', c. \tag{2h}$$

In (2c), the first derivative of the inverse demand function associated with the trade volume of exporters and their conjectural variations, is given as:

$$\frac{\partial P_{mc}(Q_{mc}, Q_{m'c})}{\partial Q_{mc}} = P'_{mc}(Q_{mc}, Q_{m'c}, \mu_{mm'c}) \quad \forall m, c. \tag{2i}$$

Given that the conjectural variations are constant, the competition pattern in the market can be determined. Substitute (2i) into (2c), we can obtain the necessary condition for the optimal solution of problem (2a) as:

$$0 \leq Q_{mc} \perp \left[PC_c + TC_{mc} + \gamma_{mc}^{QC} + \frac{\gamma^{NC}}{\overline{MV}_{mc}} - \frac{\sigma c_c}{\overline{I}_c} P_{mc} \sum_{m' \in M \setminus m} P_{m'c}(Q_{m'c} - \mu_{mm'c} Q_{mc}) \right] \geq 0 \quad \forall m, c. \tag{2j}$$

The optimal trade volumes between exporters and importers can be solved by KKT conditions (2d), (2e) and (2j).

3.3.3. Carrier module

Both the importers and exporters in the iron ore trade have the desire to minimize their overall shipping cost. Here, we propose a shipping optimization model subject to the balance of trade volume to determine the iron ore shipment volumes across different routes ($QS_{m_oc_d}$).

$$\min_{QS_{m_oc_d}} \quad SC = \sum_{m\in M}\sum_{o\in O(m)}\sum_{c\in C}\sum_{d\in D(c)} (F_{mc} + \overline{PO}_{m_o} + \overline{PD}_{c_d}) QS_{m_oc_d}, \tag{3a}$$

$$\text{s.t.} \quad \sum_{c\in C}\sum_{d\in D(c)} QS_{m_oc_d} = QO_{m_o} \quad (\gamma_{m_o}^{SEA1}) \quad \forall m, o, \tag{3a.1}$$

$$\sum_{m\in M}\sum_{o\in O(m)} QS_{m_oc_d} = QD_{c_d} \quad (\gamma_{c_d}^{SEA2}) \quad \forall c, d, \tag{3a.2}$$

$$\sum_{o\in O(m)}\sum_{d\in D(c)} QS_{m_oc_d} = Q_{m_c} \quad (\gamma_{mc}^{SEA3}) \quad \forall m, c, \tag{3a.3}$$

where SC denotes the overall shipping cost in the international iron ore trade, $\gamma_{m_o}^{SEA1}$, $\gamma_{c_d}^{SEA2}$ and γ_{mc}^{SEA3} ($\gamma_{m_o}^{SEA1}, \gamma_{c_d}^{SEA2}, \gamma_{mc}^{SEA3} free$) are the shadow prices of constraints (3a.1), (3a.2) and (3a.3).

In the objective function, transportation cost in iron ore trade consists of overall freight charges (F_{mc}) and cargo handling charges ($\overline{PO}_{m_o}, \overline{PD}_{c_d}$) of both the origin and destination ports. Constraint (3a.1) indicates that the shipment volume ($QS_{m_oc_d}$) from origin port $o \in O(m)$ to all destination ports equals to the loading volume at the same origin port (QO_{m_o}). Constraint (3a.2) illustrates that the discharging volumes of destination port (QD_{c_d}) should be equal to the sum of the shipment volume ($QS_{m_oc_d}$) from different origin ports to the destination port $d \in D(c)$. Constraint (3a.3) indicates a balance between the trade flow and the shipment flow from origin ports of exporter m to importer c.

Since it is a linear program, the KKT conditions (3b)-(3e) are necessary and sufficient for optimality as:

$$0 \le QS_{m_oc_d} \perp \left[F_{mc} + \overline{PO}_{m_o} + \overline{PD}_{c_d} - \gamma_{m_o}^{SEA1} - \gamma_{c_d}^{SEA2} - \gamma_{mc}^{SEA3}\right] \ge 0 \quad \forall m, o, c, d, \tag{3b}$$

$$\gamma_{m_o}^{SEA1} \perp \left[\sum_{c\in C}\sum_{d\in D(c)} QS_{m_oc_d} - QO_{m_o}\right] = 0 \quad \forall m, o, \tag{3c}$$

$$\gamma_{c_d}^{SEA2} \perp \left[\sum_{m\in M}\sum_{o\in O(m)} QS_{m_oc_d} - QD_{c_d}\right] = 0 \quad \forall c, d, \tag{3d}$$

$$\gamma_{mc}^{SEA3} \perp \left[\sum_{o\in O(m)}\sum_{d\in D(c)} QS_{m_oc_d} - Q_{mc}\right] = 0 \quad \forall m, c. \tag{3e}$$

It is noticed that a freight rate corresponds to a type of ship on one route. Therefore, importers/exporters also need to determine the ship type on each route. The objective of importers/exporters is to minimize the freight charges in the trade as:

$$\min_{N_{km_oc_d}} \quad FC_{mc} = \sum_{k\in K}\sum_{o\in O(m)}\sum_{d\in D(c)} FK_{km_oc_d} N_{km_oc_d} \overline{W}_k \left\lceil \frac{\overline{OD}_k \overline{V}_k}{2\overline{L}_{m_oc_d}} \right\rceil, \tag{3f}$$

$$\text{s.t.} \quad \sum_{k\in K} N_{km_oc_d} \overline{W}_k \left\lceil \frac{\overline{OD}_k \overline{V}_k}{2\overline{L}_{m_oc_d}} \right\rceil = QS_{m_oc_d} \quad (\gamma^{SHIP1}_{m_oc_d}) \quad \forall m,o,c,d, \tag{3f.1}$$

$$\sum_{m\in M}\sum_{o\in O(m)}\sum_{c\in C}\sum_{d\in D(c)} N_{km_oc_d} = \overline{NC}_k \quad (\gamma^{SHIP2}_k) \quad \forall k, \tag{3f.2}$$

where FC_{mc} is the freight charges for iron ore shipping between exporter m and importer c, $\gamma^{SHIP1}_{m_oc_d}$ ($\gamma^{SHIP1}_{m_oc_d} free$) and γ^{SHIP2}_k ($\gamma^{SHIP2}_k \geq 0$) are the shadow prices of constraints (3f.1) and (3f.2). $\left\lceil \frac{\overline{OD}_k \overline{V}_k}{2\overline{L}_{m_oc_d}} \right\rceil$ indicates the annual voyages of k-type ships between port $o \in O(m)$ and port $d \in D(c)$.

In iron ore shipping, a ship is always fully loaded in the head haul and in ballast (non-load) in the back haul. Constraint (3f.1) ensures a balance between the capacities of all ships and the shipment volumes on the route from the port $o \in O(m)$ to the port $d \in D(c)$. Constraint (3f.2) indicates the number of k-type ships in iron ore shipping are restricted by the number of same type ships in the overall market. Because (3f) is a linear program, KKT conditions (3g) - (3i) ensure the optimality, as follows:

$$0 \leq N_{km_oc_d} \perp \left[\left(FK_{km_oc_d} - \gamma^{SHIP1}_{m_oc_d} \right) \overline{W}_k \left\lceil \frac{\overline{OD}_k \overline{V}_k}{2\overline{L}_{m_oc_d}} \right\rceil + \gamma^{SHIP2}_k \right] \geq 0 \quad \forall k,m,o,c,d, \tag{3g}$$

$$\gamma^{SHIP1}_{m_oc_d} \perp \left[\sum_{k\in K} N_{km_oc_d} \overline{W}_k \left\lceil \frac{\overline{OD}_k \overline{V}_k}{2\overline{L}_{m_oc_d}} \right\rceil - QS_{m_oc_d} \right] = 0 \quad \forall m,o,c,d, \tag{3h}$$

$$0 \leq \gamma^{SHIP2}_k \perp \left[\overline{NC}_k - \sum_{m\in M}\sum_{o\in O(m)}\sum_{c\in C}\sum_{d\in D(c)} N_{km_oc_d} \right] \geq 0 \quad \forall k. \tag{3i}$$

With above two-level optimization models, the demand in shipping market is decomposed into the number of k-type ships ($N_{km_oc_d}$) on each shipping route. To align with the demand, we split iron ore shipping market into different market segments in term of the ship type on the same shipping route. In the supply side of each segment, there is a perfect competition between carriers. The freight rate should thus be equal to the marginal cost of carriers as:

$$FK_{km_oc_d} = \frac{\overline{CT}_k \cdot 2\overline{L}_{m_oc_d}}{\overline{W}_k} + \overline{DSO}_{m_o} + \overline{DSD}_{c_d} \quad \forall m,o,c,d. \tag{3j}$$

To keep it simple, the economies of scale are not considered here. Thus, the cost of carriers can be expressed as a linear cost function of the shipment volume. In (3j), the carrier's marginal cost in a single voyage is function of the unit ship operating cost (e.g. bunker, discount and crew) and unit berthing fee at ports ($\overline{DSO}_{m_o}, \overline{DSD}_{c_d}$).

3.3.4. Port selection problem

To obtain the loading/discharging volumes (QO_{m_o}/QD_{c_d}) in carrier module, we describe the port selection mechanism of importers/exporters with an import/export volume allocation problem based on the imperfect substitution among ports (Notteboom, 2009). Broadly, importers/exporters minimize their overall port cargo handling charges through allocating their imports/exports to different destination/origin ports. For importer c and its destination port $d \in D(c)$, the cargo allocation problem can be described as (4a).

$$\min_{QD_{c_d}} \quad CHC_c = \sum_{d \in D(c)} \overline{PD}_{c_d} QD_{c_d} \tag{4a}$$

$$\text{s.t.} \quad DC_c = AD_c \left(\sum_{d \in D(c)} \delta_{c_d}^{DP} QD_{c_d}^{\sigma d_c} \right)^{\frac{1}{\sigma d_c}} \quad (\gamma_c^{DP}) \quad \forall c, \tag{4a.1}$$

where CHC_c denotes the cargo handling charges that importer c pays to its destination ports, γ_c^{DP} ($\gamma_c^{DP} free$) is the shadow price of constraint (4a.1).

(4a) is a linear objective function which minimizes the overall cargo handling charges paid by importer c. Constraint (4a.1) is a CES function which describes the imperfect substitution among different ports of importer c.

Based on the FOCs for optimality of (4a), we can obtain the discharging volumes at destination port d of importer c as:

$$QD_{c_d} = \frac{DC_c}{AD_c} \left(\frac{\delta_{c_d}^{DP}}{\overline{PD}_{c_d}} \right)^{ed_c} \left(\sum_{d \in D(c)} \left(\delta_{c_d}^{DP} \right)^{ed_c} \overline{PD}_{c_d}^{1-ed_c} \right)^{\frac{-1}{\sigma d_c}} \quad \forall c, d. \tag{4b}$$

The average cargo handling price PC_c can be given as:

$$PC_c = \frac{CHC_c}{DC_c} = \frac{1}{AD_c} \left(\sum_{d \in D(c)} \left(\delta_{c_d}^{DP} \right)^{ed_c} \overline{PD}_{c_d}^{1-edc} \right)^{1-\frac{1}{\sigma d_c}} \quad \forall c. \tag{4c}$$

Similarly, for exporters, the minimization of cargo handling charges can be described as:

$$\min_{QO_{m_o}} \quad CHM_m = \sum_{o \in O(m)} \overline{PO}_{m_o} QO_{m_o} \tag{4d}$$

$$\text{s.t.} \quad QM_m = AO_m \left(\sum_{o \in O(m)} \delta_{m_o}^{OP} QO_{m_o}^{\sigma o_m} \right)^{\frac{1}{\sigma o_m}} \quad (\gamma_m^{OP}) \quad \forall m, \tag{4d.1}$$

where CHM_m is the cargo handling charges that exporter m pays to its origin ports, γ_m^{OP} ($\gamma_m^{OP} free$) is the shadow price of constraint (4d.1).

The loading volumes at origin port o of exporter m are formulated as:

$$QO_{m_o} = \frac{QM_m}{AO_m}\left(\frac{\delta^{OP}_{m_o}}{\overline{PO}_{m_o}}\right)^{eo_m}\left(\sum_{o\in O(m)}\left(\delta^{OP}_{m_o}\right)^{eo_m}\overline{PO}^{1-eo_m}_{m_o}\right)^{\frac{-1}{\sigma o_m}} \quad \forall m, o. \tag{4e}$$

The average cargo handling price PM_m can be given as:

$$PM_m = \frac{CHM_m}{QE_m} = \frac{1}{AO_m}\left(\sum_{o\in O(m)}\left(\delta^{OP}_{m_o}\right)^{eo_m}\overline{PO}^{1-eo_m}_{m_o}\right)^{1-\frac{1}{\sigma o_m}} \quad \forall m. \tag{4f}$$

3.3.5. Market-clearing and consistency conditions

To connect the modules, the following consistency and market clearing conditions are proposed:

$$QM_m = \sum_{c\in C} Q_{mc} \quad \forall m, \tag{5a}$$

$$DC_c = \sum_{m\in M} Q_{mc} \quad \forall c, \tag{5b}$$

$$P^*_{mc} = P_{mc}(Q^*_{mc}) = \frac{\overline{I}_c \delta^d_{mc} {Q^*_{mc}}^{\sigma c_c - 1}}{\sum_{m\in M}\delta^d_{mc}{Q^*_{mc}}^{\sigma c_c}} \quad \forall m, c, \tag{5c}$$

$$F_{mc} = \frac{FC_{mc}}{Q_{mc}} \quad \forall m, c. \tag{5d}$$

Market clearing condition (5a) indicates that the overall exports of an exporter are the sum of its trade to each importer. Market clearing condition (5b) requires that the overall imports of an importer are the sum of its trade with each exporter. Market-clearing condition (5c) is to calculate the equilibrium iron ore price (P_{mc}). Consistency condition (5d) is the price function of average freight rate.

4. Solution procedure

The above model can be transformed into a Mixed Complementarity Problem (MCP) with KKT conditions of each module. It is noticed that the number of ships ($N_{km_oc_d}$) is an integer variable. Therefore, it is a discretely constrained MCP (DC-MCP). Gabriel (2017) proposed that the generic MCP can be transformed into a mixed-integer nonlinear program (MINLP) though a median function-based formulation. Referring to this, our model is reformulated as an MINLP. The complex nonlinearity of CES/CET functions in our model leads to nonconvexities of the transformed MINLP, we then need to convexify those CES/CET-based nonconvexities, and apply the OA/ER/AP (Outer-Approximation/Equality-Relaxation/Augmented-Penalty) algorithm to solve the MINLP model.

4.1. MINLP formulation of DC-MCP

Given the function F: $R^n \to R^n$, a nonnegative vector $x = (x_1, x_2, x_3, ..., x_{n_x}) \in R^{n_x}$ and a vector $y = (y_1, y_2, y_3, ..., y_{n_y}) \in R^{n_y}$, we consider a MCP as follows:

Find the entire vectors (x, y)

$$0 \le F_i(x,y) \perp x_i \ge 0 \quad \forall i \in I_x = \{1, ..., n_x\}, \tag{p1}$$

$$0 = F_j(x,y), y_j free, \quad \forall j \in I_y = \{1, ..., n_y\}. \tag{p2}$$

Consider some integer elements in vector x, which should satisfy the (p1) with the following discrete restrictions:

$$x_s \in [0, +\infty), \quad \forall s \in S_x \subset I_x. \tag{p3}$$

where S_x is the set of indices for integer variables. The solution of DC-MCP is a pair of vectors (x, y) that can solve (p1), (p2) and (p3).

The MCP (p1) and (p2) can be equivalently transformed into a problem to find the zero of median function H: $R^n \to R^n$ (Gabriel, 2017). Here, we redefine H as a minimum function to fit our model, as follows:

$$H_i(x,y) = \min[x_i, F_i(x,y)], \quad \forall i \in I_x = \{1, ..., n_x\}, \tag{p4}$$

$$H_j(x,y) = F_j(x,y), y_j free, \quad \forall j \in I_y = \{1, ..., n_y\}. \tag{p5}$$

Based on the concept of function H, we consider the following problem:

$$\min_{x,y} \quad ||H(x,y)||_1 \tag{p6}$$

$$\text{s.t.} \quad x_i \in R_+ \quad \forall i \in I_x \setminus S_x, \tag{p6.a}$$

$$x_i \in Z_+ \quad \forall i \in S_x, \tag{p6.b}$$

$$y_j \in R \quad \forall j \in I_y, \tag{p6.c}$$

where $||\cdot||_1$ is the L1 vector norm, $||H(x,y)||_1 = \sum_{i \in I_x} |H_i(x,y)| + \sum_{j \in I_y} |H_j(x,y)|$. The objective function of (p6) indicates the minimization of the Manhattan Distance of $H(x,y)$. Constraints (p6.a) and (p6.c) ensure the positive and free variables, respectively. Constraint (p6.b) ensures the integer variables. Suppose the optimal solution of (p6) is the vector pair (x^*, y^*), then it is not difficult to show that the optimal solution of (p6) can solve the DC-MCP (p1, p2 and p3) if the objective function value of (p6) is equal to *zero*. By considering the complementarity between x_i and F_i in (p4), three cases regarding $H_i(x,y)$ for each $i \in I_x$ can be recognized as follows:

$$\textbf{\textit{Case 1}}: \quad If \quad x_i - F_i(x,y) > 0, \quad then \quad H_i(x,y) = F_i(x,y)$$

$$\textbf{\textit{Case 2}}: \quad If \quad x_i - F_i(x,y) < 0, \quad then \quad H_i(x,y) = x_i$$

$$\textbf{\textit{Case 3}}: \quad If \quad x_i - F_i(x,y) = 0, \quad then \quad H_i(x,y) = x_i = F_i(x,y)$$

We have $H_j(x,y) = F_j(x,y)$ holding for each $j \in I_y$.

Accordingly, the following disjunctive inequalities can be derived based on the above cases concerning $H_i(x,y)$:

$$-M(1-b_i) \le x_i - F_i(x,y) \le Mb_i \quad \forall i \in I_x, \tag{p7}$$

$$-Mb_i \le H_i(x,y) - x_i \le Mb_i \quad \forall i \in I_x, \tag{p8}$$

$$-M(1-b_i) \le H_i(x,y) - F_i(x,y) \le M(1-b_i) \quad \forall i \in I_x, \tag{p9}$$

where b_i is a binary variable for each $i \in I_x$, and M is a suitably large, positive constant. It is easy to find that ***Case 1*** holds only if $b_i = 1$. When $b_i = 1$, (p7) implies that $x_i - F_i(x,y) \ge 0$, (p8) is redundant and (p9) implies that $H_i(x,y) - F_i(x,y) = 0$. Similarly, ***Case 2*** holds only if $b_i = 0$. For ***Case 3***, given $x_i - F_i(x,y) = 0$, (p7) is feasible when $b_i = 0$ *or* 1. When $b_i = 0$, (p8) shows that $H_i(x,y) = x_i = F_i(x,y)$ and (p9) is redundant. When $b_i = 1$, (p8) is redundant and (p9) shows that $H_i(x,y) = F_i(x,y) = x_i$. Hence, ***Case 3*** holds if $b_i = 0$ *or* 1. As for $H_j(x,y)$, there are always the equalities:

$$H_j(x,y) - F_j(x,y) = 0, \quad \forall j \in I_y. \tag{p10}$$

By adding (p7), (p8), (p9) and (p10) as the constraints, we can transform the objective function of (p6) to a smooth form.

Here we introduce two pairs of nonnegative vectors (α^+, α^-) and (β^+, β^-), where $\alpha^+, \alpha^- \in R^{n_x}$ and $\beta^+, \beta^- \in R^{n_y}$. The minimum function H can be formulated as $H_i(x,y) = \alpha^+ - \alpha^-$ $(i \in I_x)$ and $H_j(x,y) = \beta_j^+ - \beta_j^-$ $(j \in I_y)$ respectively. Then, the smooth form of (p6) can be shown as follows:

$$\min_{x,y,\alpha^+,\alpha^-,\beta^+,\beta^-,b_i} \quad \sum_{i \in I_x} \alpha_i^+ + \alpha_i^- + \sum_{j \in I_y} \beta_j^+ + \beta_j^- \tag{p11}$$

$$\text{s.t.} \quad -M(1-b_i) \le x_i - F_i(x,y) \le Mb_i \qquad \forall i \in I_x, \tag{p11.a}$$

$$-Mb_i \le \alpha_i^+ - \alpha_i^- - x_i \le Mb_i \qquad \forall i \in I_x, \tag{p11.b}$$

$$-M(1-b_i) \le \alpha_i^+ - \alpha_i^- - F_i(x,y) \le M(1-b_i) \quad \forall i \in I_x, \tag{p11.c}$$

$$\beta_j^+ - \beta_j^- - F_j(x,y) = 0 \qquad \forall j \in I_y, \tag{p11.d}$$

$$x_i \in R_+ \quad \forall i \in I_x \setminus S_x, \tag{p11.e}$$

$$x_i \in Z_+ \quad \forall i \in S_x, \tag{p11.f}$$

$$y_j \in R \quad \forall j \in I_y, \tag{p11.g}$$

$$b_i \in \{0,1\} \quad \forall i \in I_x, \tag{p11.h}$$

$$\alpha_i^+, \alpha_i^- \ge 0 \quad \forall i \in I_x, \tag{p11.i}$$

$$\beta_j^+, \beta_j^- \ge 0 \quad \forall j \in I_y. \tag{p11.j}$$

Due to nonlinear formulations existing in $F_j(x,y)$ of our model, (p11) is a mixed integer nonlinear program (MINLP). Gabriel (2017) has proved that the optimal solution $(x^*, y^*, \alpha_i^{+*}, \alpha_i^{-*}, \beta_j^{+*}, \beta_j^{-*}, b_i^*)$ to (p11) contains a vector pair (x^*, y^*) which can solve the DC-MCP (p1, p2 and p3) when the objective function value of (p11) equals to zero. Hence, the DC-MCP (p1, p2 and p3) can be transformed into a MINLP (p11).

According to the definition of DC-MCP, the solution (x^*, y^*) satisfies the the discrete constraints as well as the complementarities. For a large-scale DC-MCP (p1, p2 and p3), the MINLP (p11) generally is its relaxation problem, since the complementarities (p1 and p2) need to be relaxed so as to satisfy the discrete constraint (p3). Therefore, the optimal objective function value of (p11) is larger than zero, which implies that (x^*, y^*) is an approximate solution. When the optimal objective function value of (p11) is smaller, the (x^*, y^*) is closer to the solution of the DC-MCP (p1, p2 and p3).

In order to ensure that (x^*, y^*) can solve the DC-MCP (p1, p2 and p3), it is necessary to find the global optimal solution of MINLP (p11). As a large-scale problem, there is as yet no exact algorithm developed to solve the MINLP (p11). From our model, it can be observed that the integer variables (both $N_{km_oc_d}$ and b_i) in (p11) are separable.[1] With this feature, we apply the Outer Approximation (OA) algorithms to obtain a near optimal solution of (p11) within the acceptable tolerance, which has been demonstrated to be efficient in computing time for many instances of separable MINLP (Floudas, 1995).

However, since the complexity of CES/CET functions lead to nonconvexity in $F_i(x,y)$, the global (approximate) optimum of (p11) cannot be guaranteed with general decomposition strategy algorithms, e.g., Generalized Benders Decomposition (GBD) and Outer Approximation (OA) algorithms (Kesavan, et al., 2004). Therefore, we need to further reformulate these nonconvexities in (p11) to match the requirements of the selected algorithm.

4.2. Reformulation of the CES/CET-based nonconvexity

The nonconvexity in (p11) is caused by CES utility and CET PPF. The CES utility-based nonconvexity is from the KKT conditions in exporter module. The CET PPF-based nonconvexity is from the first order conditions of cost minimization problem in production capacity allocation.

4.2.1. CES utility-based nonconvexity

Among KKT conditions of exporter module, the complementarity relationship (2j) can be abstracted as the following nonlinear format:

$$0 \le q_i \perp \left[u_i - \sum_{i' \in I_x \setminus i} \overline{\sigma} \cdot p_i p_{i'} q_{i'} + \sum_{i' \in I_x \setminus i} \overline{\sigma} \cdot \overline{\mu}_{ii'} \cdot p_i p_{i'} q_i \right] \ge 0, \quad \forall i \in I_x. \tag{p12}$$

[1] In a slight abuse of notation, suppose x is a continuous variable, y is an integer variable, and $f(x,y)$ is a function. If y in $f(x,y)$ can be separated by a univariant function $h(y)$, as $f(x,y) = g(x) + h(y)$, we describe the integer variable y as being separable.

where q_i, u_i and p_i are positive variables, $\overline{\sigma}$ and $\overline{\mu}_{ii'}$ are positive constant. (p12) is transformed into a group of constraints in MINLP (p11) shown as follows:

$$\begin{cases} q_i - u_i + \sum\limits_{i' \in I_x \setminus i} \overline{\sigma} \cdot p_i p_{i'} q_{i'} - \sum\limits_{i' \in I_x \setminus i} \overline{\sigma} \cdot \overline{\mu}_{ii'} \cdot p_i p_{i'} q_i \leq M \cdot b_i \\ -q_i + u_i - \sum\limits_{i' \in I_x \setminus i} \overline{\sigma} \cdot p_i p_{i'} q_{i'} + \sum\limits_{i' \in I_x \setminus i} \overline{\sigma} \cdot \overline{\mu}_{ii'} \cdot p_i p_{i'} q_i \leq M(1 - b_i) \\ -M \cdot b_i \leq \alpha_i^+ - \alpha_i^- - q_i \leq M \cdot b_i \\ \alpha_i^+ - \alpha_i^- - u_i + \sum\limits_{i' \in I_x \setminus i} \overline{\sigma} \cdot p_i p_{i'} q_{i'} - \sum\limits_{i' \in I_x \setminus i} \overline{\sigma} \cdot \overline{\mu}_{ii'} \cdot p_i p_{i'} q_i \leq M(1 - b_i) \\ -\alpha_i^+ + \alpha_i^- + u_i - \sum\limits_{i' \in I_x \setminus i} \overline{\sigma} \cdot p_i p_{i'} q_{i'} + \sum\limits_{i' \in I_x \setminus i} \overline{\sigma} \cdot \overline{\mu}_{ii'} \cdot p_i p_{i'} q_i \leq M(1 - b_i) \\ \forall i, i' \in I_x, \quad i \neq i', \end{cases} \tag{p13}$$

where M is positive, $b_i \in \{0, 1\}$, $\alpha_i^+ \in \alpha^+$ and $\alpha_i^- \in \alpha^-$. The nonlinear terms $\overline{\sigma} \cdot p_i p_{i'} q_{i'}$ and $\overline{\sigma} \cdot \overline{\mu}_{ii'} \cdot p_i p_{i'} q_i$ are nonconvex. We can firstly linearize the (p13) by introducing two positive variables $\phi_{ii'}$ and $\omega_{ii'}$ to replace the nonlinear terms, as:

$$\phi_{ii'} = \overline{\sigma} \cdot p_i p_{i'} q_{i'}, \qquad \forall i, i' \in I_x, \quad i \neq i', \tag{p14}$$

$$\omega_{ii'} = \overline{\sigma} \cdot \overline{\mu}_{ii'} p_i p_{i'} q_i, \qquad \forall i, i' \in I_x, \quad i \neq i'. \tag{p15}$$

Since $\overline{\sigma}$ and $\overline{\mu}_{ii'}$ are positive, the right-hand sides of (p14) and (p15) are posynomials which can be convexified though an exponential transformation, as:

$$\phi_{ii'} = \overline{\sigma} \cdot e^{\tau_i^p + \tau_{i'}^p + \tau_{i'}^q}, \quad \forall i, i' \in I_x, \quad i \neq i', \tag{p16}$$

$$\omega_{ii'} = \overline{\sigma} \cdot \overline{\mu}_{ii'} e^{\tau_i^p + \tau_{i'}^p + \tau_i^q}, \quad \forall i, i' \in I_x, \quad i \neq i', \tag{p17}$$

$$\tau_i^p = \ln p_i, \quad \forall i \in I_x, \tag{p18}$$

$$\tau_i^q = \ln q_i, \quad \forall i \in I_x, \tag{p19}$$

where τ_i^p and τ_i^q are free. It is easy to prove that the right-hand sides of (p16) and (p17) are convex, $\ln p_i$ and $\ln q_i$ are concave. Based on (p14)-(p19), the constraint group (p13) can be reformulated

as the following convex format (p20):

$$\begin{cases} q_i - u_i + \sum\limits_{i' \in I_x \backslash i} \phi_{ii'} - \sum\limits_{i' \in I_x \backslash i} \omega_{ii'} \leq M \cdot b_i \\ -q_i + u_i - \sum\limits_{i' \in I_x \backslash i} \phi_{ii'} + \sum\limits_{i' \in I_x \backslash i} \omega_{ii'} \leq M(1 - b_i) \\ -M \cdot b_i \leq \alpha_i^+ - \alpha_i^- - q_i \leq M \cdot b_i \\ \alpha_i^+ - \alpha_i^- - u_i + \sum\limits_{i' \in I_x \backslash i} \phi_{ii'} - \sum\limits_{i' \in I_x \backslash i} \omega_{ii'} \leq M(1 - b_i) \\ -\alpha_i^+ + \alpha_i^- + u_i - \sum\limits_{i' \in I_x \backslash i} \phi_{ii'} + \sum\limits_{i' \in I_x \backslash i} \omega_{ii'} \leq M(1 - b_i) \\ \overline{\sigma} \cdot e^{\tau_i^p + \tau_{i'}^p + \tau_{i'}^q} - \phi_{ii'} = 0 \\ \overline{\sigma} \cdot \overline{\mu}_{ii'} e^{\tau_i^p + \tau_{i'}^p + \tau_i^q} - \omega_{ii'} = 0 \\ \tau_i^p - \ln p_i = 0 \\ \tau_i^q - \ln q_i = 0 \\ \phi_{ii'}, \omega_{ii'} \in R_+, \quad \tau_i^p, \tau_i^q \in R \\ \forall i, i' \in I_x, \quad i \neq i'. \end{cases} \tag{p20}$$

4.2.2. CET production possibility frontier-based nonconvexity

In exporter module, we endogenize the export capacity through a cost minimization problem under the constraint of CET production possibility frontier. The FOC of this problem can be abstracted as the following format:

$$k_j = \overline{\rho} \cdot \overline{\delta}_j \cdot t_j^{-\overline{\varepsilon}} \left(\sum_{j \in I_y} \overline{\delta}_j \cdot t_j^{1-\overline{\varepsilon}} \right)^{\frac{\overline{\varepsilon}}{1-\overline{\varepsilon}}}, \quad \forall j \in I_y, \tag{p12}$$

where k_j and t_j are positive variables, $\overline{\rho}$ and $\overline{\delta}_j$ are positive constants, and ε is a negative constant. (p21) can be transformed into a constraint of MINLP (P11), which is shown as:

$$\beta_j^+ - \beta_j^- - k_j + \overline{\rho} \cdot \overline{\delta}_j \cdot t_j^{-\overline{\varepsilon}} \left(\sum_{j \in I_y} \overline{\delta}_j \cdot t_j^{1-\overline{\varepsilon}} \right)^{\frac{\overline{\varepsilon}}{1-\overline{\varepsilon}}} = 0, \quad \forall j \in I_y, \tag{p22}$$

where $\beta_j^+ \in \beta^+$, $\beta_j^- \in \beta^-$. The nonlinear term in the equality (p22) is nonconvex. To convexify the (p22), we firstly introduce a positive variable ψ, by

$$\psi = \sum_{j \in I_y} \overline{\delta}_j \cdot t_j^{1-\overline{\varepsilon}}, \tag{p23}$$

$$\beta_j^+ - \beta_j^- - k_j + \overline{\rho} \cdot \overline{\delta}_j \cdot t_j^{-\overline{\varepsilon}} \psi^{\frac{\overline{\varepsilon}}{1-\overline{\varepsilon}}} = 0, \quad \forall j \in I_y. \tag{p24}$$

It can be proved that the right-hand side of (p23) is convex when $\overline{\varepsilon} < 0$. Since the nonlinear term in (p24) is a posynomial, it can be convexified through an exponential transformation, as:

$$\beta_j^+ - \beta_j^- - k_j + \overline{\rho} \cdot \overline{\delta}_j \cdot \exp\left(-\overline{\varepsilon} \cdot \theta_j^t + \frac{\overline{\varepsilon}}{1-\overline{\varepsilon}} \cdot \theta^\psi\right) = 0, \quad \forall j \in I_y, \tag{p25}$$

$$\theta_j^t = \ln t_j, \quad \forall j \in I_y, \tag{p26}$$

$$\theta^\psi = \ln \psi, \tag{p26}$$

where θ_j^t and θ^ψ are free. Based on (p23), (p25), (p26) and (p27), the constraint (p22) can be reformulated as a group of convex constraints:

$$\begin{cases} \beta_j^+ - \beta_j^- - k_j + \overline{\rho} \cdot \overline{\delta}_j \cdot \exp\left(-\overline{\varepsilon} \cdot \theta_j^t + \frac{\overline{\varepsilon}}{1-\overline{\varepsilon}} \cdot \theta^\psi\right) = 0 \\ \theta_j^t - \ln t_j = 0 \\ \theta^\psi - \ln \psi = 0 \\ \sum\limits_{j \in I_y} \overline{\delta}_j \cdot t_j^{1-\overline{\varepsilon}} - \psi = 0 \\ \psi \in R_+, \quad \theta_j^t, \theta^\psi \in R \\ \forall j \in I_y. \end{cases} \tag{p28}$$

By convexifying these non-convex terms, MINLP (p11) can be reformulated as follows:

$$\min_{x,y,\alpha^+,\alpha^-,\beta^+,\beta^-,b_i} \quad f(\alpha_i^+, \alpha_i^-, \beta_j^+, \beta_j^-) \tag{p29}$$

$$\text{s.t.} \quad g(x, y, \alpha^+, \alpha^-, \beta^+, \beta^-, b_i) \leq 0 \tag{p29.a}$$

$$h(x, y, \alpha^+, \alpha^-, \beta^+, \beta^-, b_i) = 0 \tag{p29.b}$$

$$x_i \in R_+ \quad \forall i \in I_x \setminus S_x, \tag{p29.c}$$

$$x_i \in Z_+ \quad \forall i \in S_x, \tag{p29.d}$$

$$y_j \in R \quad \forall j \in I_y, \tag{p29.e}$$

$$b_i \in \{0, 1\}, \quad \forall i \in I_x, \tag{p29.f}$$

$$\alpha_i^+, \alpha_i^- \geq 0 \quad \forall i \in I_x, \tag{p29.g}$$

$$\beta_j^+, \beta_j^- \geq 0 \quad \forall j \in I_y. \tag{p29.h}$$

where both $g(\cdot)$ and $h(\cdot)$ are either linear or convex. The OA/ER/AP algorithm proposed by Viswanathan et al. (1990) can be applied to solve the MINLP (p29). The global optimal solution of (p29) contains the vector pair $(x*, y*)$, which is the relaxed solution to DC-MCP (p1, p2 and p3).

5. Scenario simulation

In this section, we conduct a case study for the international ore market based on our model. Through simulating the scenarios of large-size fleet expansion, we explore the impact of large-size ship adoption on the iron ore trade. The model is solved using the DICOPT Solver of GAMS.

5.1. Case setting

According to the database released by UN Comtrade in 2016, China, Japan and South Korea accounted for 81.7% of total international iron ores import in 2015. Australia and Brazil enjoyed an over 81% share of global exports in the same year. Therefore, we conduct our case study on the trade among them, as shown in Table 5.

Table 5 Main importers and exporters in iron ore trade

Set	Subscript	Element	Explanation
C	c	$c1$	China
		$c2$	Japan
		$c3$	South Korea
M	m	$m1$	Brazil
		$m2$	Australia

Table 6 Origin/destination ports of main exporters/importers

Set	Subscript	Element	Explanation
$O(m1)$	o	$o1$	Port PDM
		$o2$	Ports of Victoria (main Tubarao and UBU)
		$o3$	Ports of Rio de Janeiro (main CSN, CPBS and GIT)
$O(m2)$	o	$o4$	Pilbara port authority (main Dampier and Port Headland)
		$o5$	Other non-authority ports (e.g., Walcott and Cape Preston)
$D(c1)$	d	$d1$	Ports in North of China
		$d2$	Ports in Yangtze River Delta
		$d3$	Ports in South of China
$D(c2)$	d	$d4$	Ports of Japan
$D(c3)$	d	$d5$	Ports of South Korea

Table 7 Types of Capesize ships in the iron ore shipping market

Set	Subscript	Element	Explanation
K	k	$k1$	Small size- 150,000-200,000 dwt
		$k2$	Medium size- 200,000-300,000 dwt
		$k3$	Large size- 300,000-400,000 dwt

In Brazil, the main iron ore loading ports include Port of PDM, Port Victoria (e.g. Tubarao) and Port Rio de Janerio (e.g. CSN terminal). The majority of Australian iron ore is exported from ports located in Western Australia, e.g., Port Dampier and Port Headland under Pilbara Port Authority. It is worth noticing that some ports in Western Australia accounting for a considerable amount of export are owned and operated by iron ore miners (e.g. Port Walcott). we divide the iron ore export ports of Australia into Pilbara Ports Authority and miner dedicated ports. For the loading ports in China, we simply divide them into three port groups according to their geographical proximity, these being North of China, Middle China and South of China. As for Japan and South Korea, we assume each of them has only one iron ore port because their iron ore discharging ports are quite concentrated. Table 6 shows the details of origin/destination ports considered in our model.

The Capesize ship is the mostly adopted ship type for transporting iron ore. The tonnage of Capesize ships varies greatly. Simply, we classify Capesize ships (the type of carriers) into three types, as shown in table 7.

5.2. Data and parameter estimation

The data applied in this study is collected from multiple sources. Due to the delayed nature of updating port data (only data of 2015 is available at present for some ports, e.g., CSN and GIT terminals in Brazil), the data we used in this study is all based on the year 2015.

Among the data, the iron ore purchasing budgets and export capacities are derived from *UN Comtrade*. Iron ore production cost is collected from *MySteel.com*. Port charges are derived from the corresponding websites of Port Authorities. Fleet capacities and average DWTs are obtained from *Shipping Intelligence Network*. Sea route distances between origin and destination ports are from *Sea-Distances.Org*. Ship operating cost, ship speed and average annual operating days of ships are provided by the *COSCO Bulk*. Detailed values of the above data are provided in Appendix A.

In this study, we need to estimate the parameters of CES functions. We adopt the linear regression approach proposed by Gallaway et al. (2003) to estimate parameters of the CES utilities of importers and the CET production possibility frontier of exporters. This estimation is based on monthly import volumes between ODs and corresponding CIF prices. The data is from *MySteel.com*, covering the period from January 2014 to December 2016.

The parameters of CET PPF are estimated using the Kmenta approximation approach adopted by Koesler and Schymura (2015). This estimation is built on the monthly iron ore export volumes among ODs during January 2014 to December 2016. The data is collected from *MySteel.com*.

The parameters of CES functions in the import/export volume allocation problem are also estimated based on the Kmenta approximation approach. This estimation is based on the iron ore loading/discharging volumes of origin/destination ports presented in Table 6. Data of Brazilian ports is collected from *LBH Group*. Data of Australian ports is obtained from *trade statistics of Western Australia Port Authorities*. Data on discharging volumes at China ports is derived from *Chinas Customs Statistics*. The data used for estimation is also on the monthly basis, covering the period from January 2014 to December 2016.

We also need to estimate the parameter in the conjectural variations of exporters. Here, we apply the approach proposed by Santis et al. (2002). Detailed information regarding the parameter estimation is provided in Appendix B.

Table 8 Scenarios of increasing the number of large ships in Brazil

Scenario	The number of large-size ships
T0	0
T10	10
T20	20
T30	30
T40	40
T50	50
T60	60
T70	70
T80	80
T90	90
T100	100
T110	110
T120	120
T130	130
T140	140
T150	150
T160	160
T170	170

5.3. Simulation the impact of larger ships on iron ore trade volume

Based upon our model, we assess the impact of large-size ships (hereafter, large ships) on the international iron ore trade through simulating the scenarios. The scenarios are constructed using data from 2015. In 2015, the iron ore shipping market was characterized by overcapacity, and the freight rate reached its historical low point. Brazil adopted large ships, but Australia didnt, due to limitations on the depth of its ports. To begin with, we set up the benchmark of the scenarios by making the number of large ships ($k3$) equal to zero. Based on this benchmark, we create 17 scenarios by adding ten large ships at a time. The scenarios are shown in Table 8.

Among the scenarios, T60 is consistent with the real situation of the international iron ore market in 2015. In Table 9, we compare the simulated trade volume and trade price from scenario T60 with the actual figures from 2015, and find they are close to each other, which proves the validity of our model.

In the exporter module, the complementary relationship (2j) for the optimal solution of problem (2a) represents the reaction function of the exporter in the Cournot competition. It implies that the trade volume from exporter m to importer c, except for the influence of rivals, is also affected by the following factors: a) the cargo handling price at discharge ports of the importer (PC_c); b) the trade cost of the exporter (TC_{mc}); c) the shadow price (γ_{mc}^{QC}) in constraint (2a.1), indicating restriction of the export capacity QC_{mc} (higher γ_{mc}^{QC} indicates a higher export restriction of exporter m to importer c); d) the restriction of the fleet capacity ($\gamma^{NC}/\overline{MV}_{mc}$), presented by the ratio of the shadow price (γ^{NC}) of constraint (2a.2) and the average voyages ($\overline{MV}_{mc}$). Let

Table 9 Comparison between simulated results and actual values from 2015

ODs	Indicators			
	Trade volume[a] (Q_{mc})		Trade price[b] (P_{mc})	
	Result of T60	Real data of 2015[c]	Result of T60	Real data of 2015[d]
$m1$-$c1$	1695.59	1784.47	64.94	62.98
$m1$-$c2$	330.78	345.48	77.02	78.66
$m1$-$c3$	110.66	97.04	79.65	79.69
$m2$-$c1$	6231.92	6283.92	59.10	58.92
$m2$-$c2$	891.87	875.04	61.32	64.53
$m2$-$c3$	582.92	574.70	58.85	63.35

Note: (a) The unit of trade volume is 10^6 tonnes. (b) The unit of trade price is \$\tonne. (c) The real data related to the trade volume in 2015 comes from *Mysteel.com*. (d) The real data related to the trade price in 2015 is collected from *UN Comtrade*.

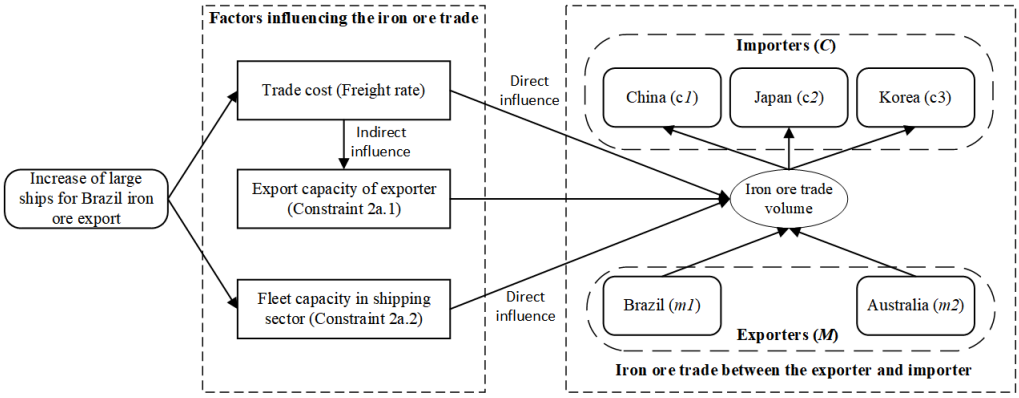

Figure 2 Fundamentals of the influence in iron ore trade by increasing large ships

η_{mc} denote the restriction of fleet capacity in the trade between exporter m and importer c, then $\eta_{mc} = \gamma^{NC}/\overline{MV}_{mc}$. Higher η_{mc} indicates a higher restriction of fleet capacities to the trade between exporter m and importer c.

When the large ship is adopted, the cargo handling price stays fixed, but the other three factors will determine the trade volume. The first is the trade cost. Since the marginal voyage cost of large ships is lower than that of small ones, the adoption of large ships can lower the freight rate, thus saving on trade costs and increasing the trade volume. The second is the restriction of export capacity. The export capacity is related to the trade costs of the exporter. Reduction in trade costs will affect the export capacity, which may lead to a change of trade volume. The third is the restriction of fleet capacity. The adoption of large ships increases the fleet capacity, which frees its restriction over trade volume when the market is good. Figure 2 shows the fundamentals of the influence on iron ore trade by increasing the number of large ships.

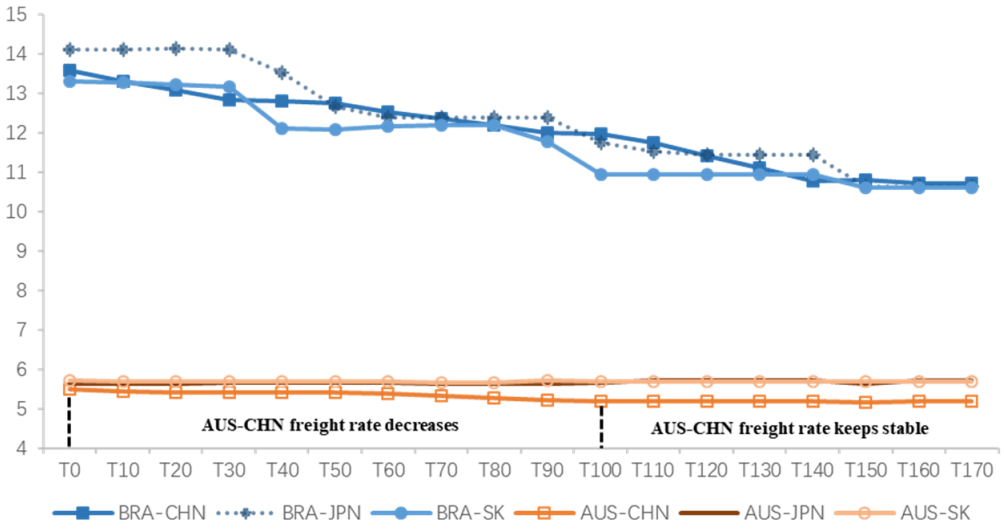

Figure 3 Average freight rates between exporters and importers (unit: $/tonne)

Next, based on the simulation results, we analyze how the above three factors affect the trade volume along with the increasing number of large ships used in Brazilian iron ore exports.

Figure 3 shows the change in freight rates. Freight rates for the Brazil-East Asia routes drop significantly with the increase in the number of large ships, while little decline is observed on the Australia-East Asia routes. In particular, the freight rates remain almost unchanged for the routes from Australia to Japan and South Korea. As for the freight rate from Australia to China, below T100, the increase in number of large ships shifts mid-size ships from the Brazil-East Asia routes to the Australia-China route. This leads to a reduction in freight rate on the Australia-China route. Above T100, the available mid-size ships for Australia reduces, and as a result the increase in number of large ships has only a minor impact on the freight rate of the Australia-China route.

Table 10 presents the changes in restrictions from the export capacity and the fleet capacity. For the restriction of export capacity, γ_{m1c}^{QC} remains at zero with the increasing number of large ships, indicating that Brazil has no restriction on trade with East Asia. γ_{m2c1}^{QC} is zero, indicating that Australia has no restrictions on exports to China. γ_{m2c2}^{QC} and γ_{m2c3}^{QC} are positive, indicating that Australia has restrictions over export capacity affecting the imports into Japan and South Korea. As for the restriction of fleet capacity, $\eta_{mc} \geq 0$ during the T0 to T50 phase, which indicates that all Brazilian and Australian trades with East Asia are restricted by fleet capacities. As the number of Brazilian large ships increases, η_{mc} decreases, showing that the insufficiency of fleet capacity is continuously eased. After T50, $\eta_{mc} = 0$, suggesting that the fleet capacity in shipping market is excessive.

Knowing the changes of the above three factors, we can analyze the impact of large ship on the trade volumes in term of the ODs.

Table 10 Degree of restriction of export capacities and fleet capacities

Scenario	Restriction degree of export capacities (γ_{m2c}^{QC})				Restriction degree of fleet capacities ($\eta_{mc} = \gamma^{NC}/MV_{mc}$)			
	$m1$-c[a]	$m2$-$c1$	$m2$-$c2$	$m2$-$c3$	$m1$-c	$m2$-$c1$	$m2$-$c2$	$m2$-$c3$
T0	0	0	0	8.47	10.57	3.40	3.52	3.38
T10	0	0	0.27	7.61	8.11	2.62	2.70	2.60
T20	0	0	0.68	6.83	5.86	1.89	1.95	1.87
T30	0	0	1.05	6.12	3.79	1.22	1.26	1.21
T40	0	0	1.30	4.85	1.92	0.62	0.64	0.62
T50[b]	0	0	1.49	4.28	0.19	0.06	0.06	0.06
T60	0	0	1.44	4.21	0	0	0	0
T70	0	0	1.39	4.18	0	0	0	0
T80	0	0	1.34	4.15	0	0	0	0
T90	0	0	1.29	3.90	0	0	0	0
T100	0	0	1.13	3.34	0	0	0	0
T110	0	0	1.07	3.34	0	0	0	0
T120	0	0	1.07	3.34	0	0	0	0
T130	0	0	1.07	3.33	0	0	0	0
T140	0	0	1.07	3.33	0	0	0	0
T150	0	0	0.94	3.17	0	0	0	0
T160	0	0	0.94	3.17	0	0	0	0
T170	0	0	0.94	3.17	0	0	0	0

Note: (a) c denotes every importer (China, Japan and South Korea); (b) Shortage of fleet capacities exists before T50 and overcapacities occur after T50.

5.3.1. Trade volumes to Chinese iron ore market

Table 10 shows that iron ore exports from both Brazil and Australia to China are not restricted by export capacity. Rather, trade volume is determined by the freight rate and the restriction from fleet capacity. Between T0 and T100, the freight rate from Brazil and Australia to China decreases. Above T100, although the freight rate from Brazil to China still decreases, that from Australia to China remains unchanged. As for the restriction of fleet capacity, below T50 the fleet capacity from both Australia and Brazil to China is in short supply, which causes a restriction on trade volume from both Brazil and Australia in the Chinese market. Above T50, the fleets from both Brazil and Australia to China have overcapacity. Combining the impact of freight rate and restriction of fleet capacity, we divide the impact of increasing the number of large ships in the Chinese iron ore market into three phases:

In the T0-T50 phase, the shipping market is in short of fleet capacity and the freight rates from both Brazil and Australia to China decrease. Along with the increase in the number of large ships, the synergy of increasing the fleet capacity and freight rate reduction leads to the growth of trade volume from both Brazil and Australia to the Chinese market. As shown in Figure 4, in this phase, the trade volume of Brazil and Australia to China increased by 54.203 and 26.852 million tonnes, respectively.

In the T50-T100 phase, the fleet has overcapacity and the freight rates from both Brazil and Australia decrease. Figure 4 shows that in this phase the growth rate for both trade from Australia

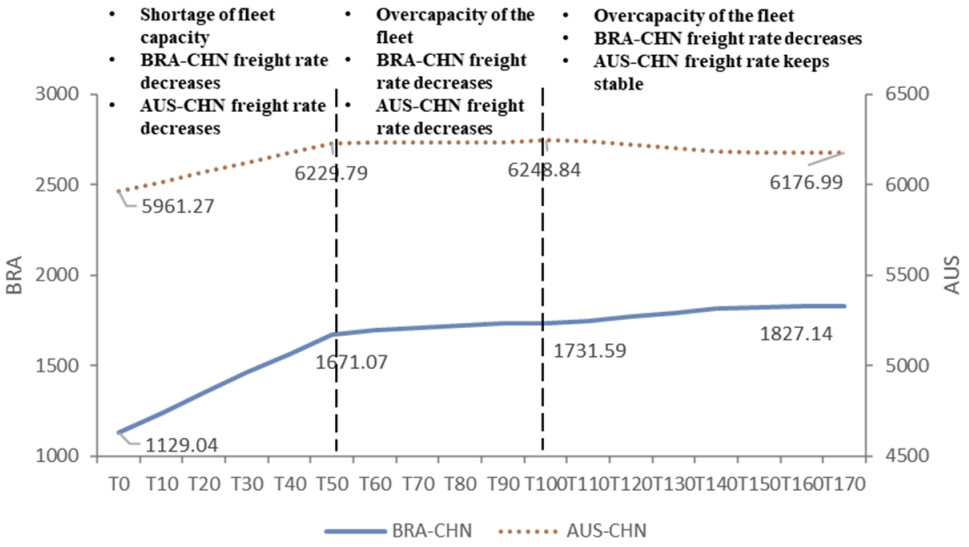

Figure 4 **Iron ore trade volumes in Chinese market (unit: 100 thousand tonnes)**

and from Brazil to China largely slows down. This result suggests that lowering the freight rate has limited effect on the growth of trade volume. Combining this result with that of the T0-T50 phase, we find that the main driving force behind the rapid growth in trade volume is not the decline in freight rates, but the growth potential released by easing the restriction of fleet capacity when the shipping market is in short supply.

In the T100-T170 phase, the fleet maintains a state of overcapacity. The freight rate on the route from Brazil to China decreases, but that on the route from Australia to China barely changes. In this phase, the Brazilian trade volume with China increases by 9.5 million tonnes, while the Australian trade volume decreases by 6 million tonnes. This is because, above T100, the freight rate on the Australia-China route remains stable but the freight rate on the Brazil-China route continues to decrease. As a result, the disadvantage of Brazils trade costs compared to Australia becomes smaller. Given Chinas fixed budget, Australia needs to reduce its iron ore price to expand its trade volume with China, while this will lead to a decline in its profit margins. To minimize its profit loss, Australia has to maintains its iron ore price, but then its trade volume declines.

5.3.2. Trade volumes to Japanese and South Korean iron ore market

Figure 5 presents the changes in trade volume to the Japanese and South Korean markets. According to changes in the three factors presented in Table 10, Brazil's trade volume associated with Japan and South Korea is not restricted by its export capacity. With the increase in number of large ships, the freight rates on the Brazil-Japan/Brazil-South Korea shipping routes decrease. As

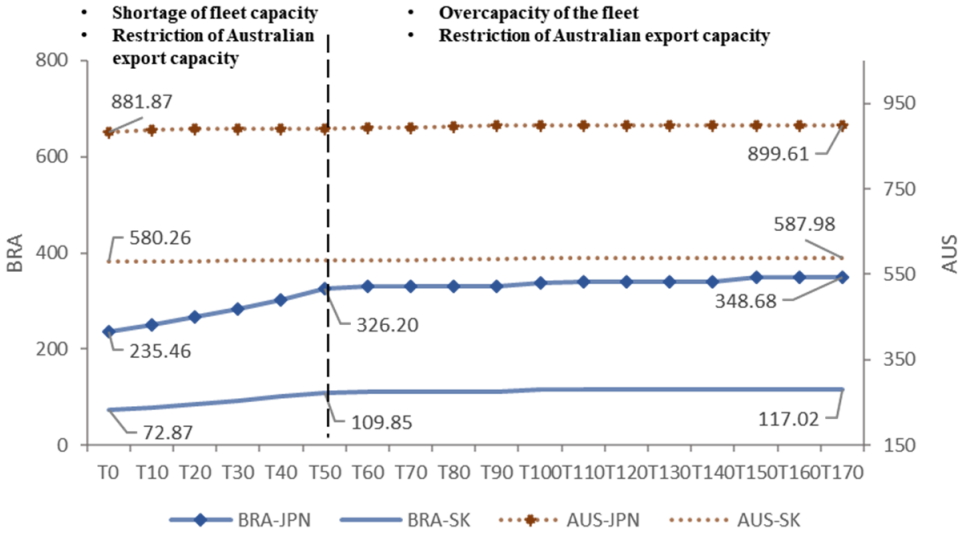

Figure 5 **Iron ore trade volumes in Japanese and South Korea market (unit: 100 thousand tonnes)**

for the restriction of fleet capacity, below T50, the shortage of fleet capacity gets mitigated, and above T50, overcapacity of the fleet appears.

Referring to the analysis of the Chinese market, alleviating the shortage of fleet capacity is the main factor driving the growth in trade volume. Therefore, the trends of Brazilian trade volume with Japan and South Korea are basically in line with the Brazil-China trade trends. In the phase T0-T50, where the fleet has a shortage of capacity, increasing the number of large ships can effectively promote a growth in trade volume between Brazil and Japan/South Korea. In the phase T50-T170 where there is overcapacity of the fleet, the increase in number of large ships has minor impact on the trade volume of Brazil with Japan and South Korea.

During the whole T0 to T170 period, the trade volume of Australia with Japan and South Korea is unchanged. Thus, the change in trade volume of Australia with Japan and South Korea is different from that with China. This is due to the fact that the freight rates on the routes between Australia and Japan/South Korea remain stable (Figure 3). More intriguingly, Australia's export capacity to Japan and South Korea is always restricted (Table 10), which indicates that the trade volume can only equal to the export capacity, no matter whether the shortage of fleet capacity is relieved or not. Therefore, as the number of large ships increase, the trade volume growth between Australia and Japan/South Korea is insignificant. From T0 to T170, the trade volume of Australia with Japan only increases by 1.77 million tonnes, while that with South Korea only increases by 773,000 tonnes.

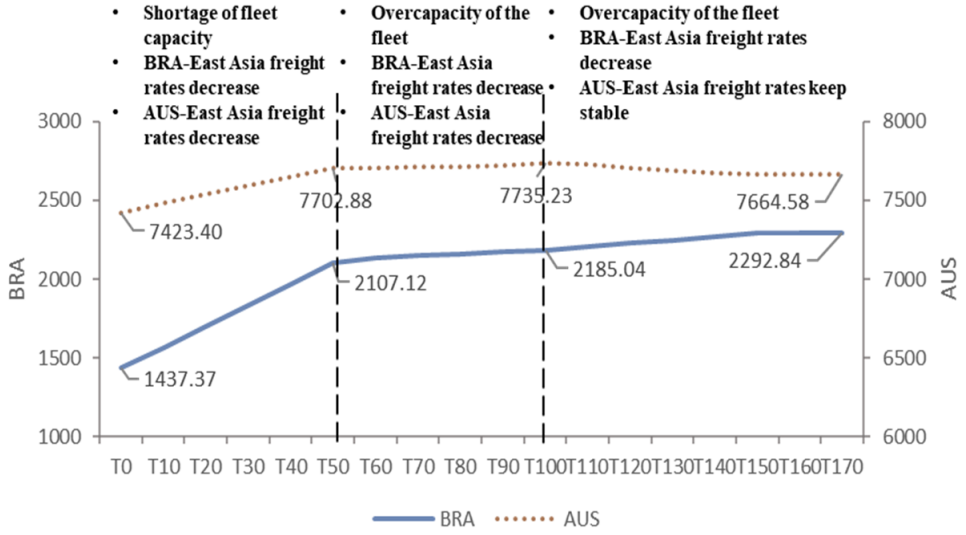

Figure 6 Overall iron ore imports into East Asia from Brazil and Australia (unit: 100 thousand tonnes)

5.3.3. summary

Figure 6 shows the overall iron ore trade changes on the proposed OD pairs, these being highly consistent with the changes in Chinese market. Where there is a shortage of fleet capacity, increasing the number of large ships in Brazil can significantly improve the trade volume for both Brazil and Australia. When there is overcapacity of the fleet, increasing the number of large ships only leads to a reduction in freight rates, which has limited impact on trade volume. In the case of fleet overcapacity, only when the freight rate on the Australia-East Asia route is stable (e.g., during the T100-T170 phase), can the increase in the number of large ships benefit Brazil in the market competition.

According to the above results, we can understand why deploying more large ships was actually inefficient for Brazilian iron ore exports. Since 2008, due to insufficient fleet capacity in iron ore shipping and the optimistic market expectation of iron ore demand in East Asia, Brazilian iron ore giant Vale signed thirty-five newbuilding contracts for the 400,000-tonne Valemax in order to reverse its competitive disadvantage in the East Asian iron ore market. As expected, the application of Valemax fleet would bring about a rapid growth in trade volume at a time when the market was clearly short of fleet capacity (T0-T50 phase). However, when the first Valemax was launched in November 2011, the shipping market declined, the freight rate was at its historically low level, and fleet overcapacity appeared. The T50-T100 phase emerged as more Valemax ships were delivered between 2012 and 2015. This increasing number of large ships further lowered the freight rate, which was already low. Hence, the impact of large ships on trade volume is insignificant. In fact,

Brazils trade volume in the East Asian market during this period increased by only 10% (UN Comtrade, 2016).

6. Conclusion

In this paper, we have established a mixed complementarity-based equilibrium model to analyze the impact of shipping on the international iron ore trade. This model builds upon the previous literature through developing a more plausible utility-derived demand function, describing a more realistic oligopolistic market structure, and endogenizing the export capacity of exporters. To understand the interaction between the iron ore trade and the shipping sector, this model also constructs a shipping module by taking into account the strategies of carriers.

The integer variables in the carrier module make this model difficult to be solved, since traditional MCP algorithms are non-applicable, having discrete constraints. To overcome this, we have provided a solution procedure. We have first transformed the model into a nonconvex MINLP. Then, an exponential transformation is applied to convexify the nonconvexities depending on their posynomial features. The final convex MINLP is solved by an OA/ER/AP algorithm.

We have also conducted a scenario simulation based on real data from 2015 to examine the impact of large ship adoption on the iron ore trade. We find that although adopting large ships can reduce the shipping cost of exporters, it hardly affects their trade volumes. In contrast, the restriction of fleet capacity is the dominant factor determining the iron ore trade volume. However, when the iron ore market is good and fleet capacity is in short supply, then increasing the number of large ships can ease the strain on fleet capacity, which can be effective in promoting an increase in trade volume.

References

Assembayeva, Makpal, Jonas Egerer, Roman Mendelevitch, and Nurkhat Zhakiyev. "A spatial electricity market model for the power system: The Kazakhstan case study." *Energy* 149 (2018): 762-778.

Australia, Western Port Authority. *Trade statistics.* The Authority., 2015.

Bai, Xiwen, and Jasmine Siu Lee Lam. "An integrated analysis of interrelationships within the very large gas carrier (VLGC) shipping market." *Maritime Economics and Logistics* 21, no. 3 (2019): 372-389.

Boots, Maroeska G., Fieke AM Rijkers, and Benjamin F. Hobbs. "Trading in the downstream European gas market: a successive oligopoly approach." *The Energy Journal* (2004): 73-102.

China Customs Statistical Yearbook of 2018.

Comtrade, U. N. "International Trade Statistics Database (2016)." (2018).

De Santis, Roberto A. "A conjectural variation computable general equilibrium model with free entry." *Policy Evaluation with Computable General Equilibrium Models, Routledge, London* (2002).

Distances, Sea. "Sea Distances." *Org: [sn]* (2015).

Egerer, Jonas, Friedrich Kunz, and Christian Von Hirschhausen. "Development scenarios for the North and Baltic Seas GridCA welfare economic analysis." *Utilities Policy* 27 (2013): 123-134.

Egerer, Jonas, Jens Weibezahn, and Hauke Hermann. "Two price zones for the German electricity market-Market implications and distributional effects." *Energy Economics* 59 (2016): 365-381.

Egging, Ruud, Franziska Holz, and Steven A. Gabriel. "The World Gas Model: A multi-period mixed complementarity model for the global natural gas market." *Energy* 35, no. 10 (2010): 4016-4029.

Floudas, Christodoulos A. *Nonlinear and mixed-integer optimization: fundamentals and applications.* Oxford University Press, 1995.

Gabriel, Steven A. "Solving discretely constrained mixed complementarity problems using a median function." *Optimization and Engineering* 18, no. 3 (2017): 631-658.

Gabriel, Steven A., Jifang Zhuang, and Supat Kiet. "A large-scale linear complementarity model of the North American natural gas market." *Energy economics* 27, no. 4 (2005a): 639-665.

Gabriel, Steven A., Supat Kiet, and Jifang Zhuang. "A mixed complementarity-based equilibrium model of natural gas markets." *Operations Research* 53, no. 5 (2005b): 799-818.

Gallaway, Michael P., Christine A. McDaniel, and Sandra A. Rivera. "Short-run and long-run industry-level estimates of US Armington elasticities." *The North American Journal of Economics and Finance* 14, no. 1 (2003): 49-68.

Germeshausen, Robert, Timo Panke, and Heike Wetzel. "Firm characteristics and the ability to exercise market power: empirical evidence from the iron ore market." *Empirical Economics* (2018): 1-25.

Hecking, Harald, and Timo Panke. "The global markets for coking coal and iron oreComplementary goods, integrated mining companies and strategic behavior." *Energy Economics* 52 (2015): 26-38.

Holz, Franziska, Philipp M. Richter, and Ruud Egging. "The Role of Natural Gas in a Low-Carbon Europe: Infrastructure and Supply Security." *Energy Journal* 37 (2016).

Huppmann, Daniel. "Endogenous production capacity investment in natural gas market equilibrium models." *European Journal of Operational Research* 231, no. 2 (2013): 503-506.

Janda, Karel, Jan Malek, and Lukas Recka. *Influence of Renewable Energy Sources on Electricity Transmission Networks in Central Europe.* No. 05/2017. IES Working Paper, 2017.

Kesavan, Padmanaban, Russell J. Allgor, Edward P. Gatzke, and Paul I. Barton. "Outer approximation algorithms for separable nonconvex mixed-integer nonlinear programs.." *Mathematical Programming* 100, no. 3 (2004): 517-535.

Klemperer, Paul D., and Margaret A. Meyer. "Supply function equilibria in oligopoly under uncertainty." *Econometrica: Journal of the Econometric Society* (1989): 1243-1277.

Koesler, Simon, and Michael Schymura. "Substitution elasticities in a constant elasticity of substitution frameworkCempirical estimates using least squares." *Economic Systems Research* 27, no. 1 (2015): 101-121.

Kunz, Friedrich, and Alexander Zerrahn. "Benefits of coordinating congestion management in electricity transmission networks: Theory and application to Germany." *Utilities Policy* 37 (2015): 34-45.

Leuthold, Florian, Ina Rumiantseva, Hannes Weigt, Till Jeske, and Christian Von Hirschhausen. "Nodal Pricing in the German Electricity Sector-A Welfare Economics Analysis, with Particular Reference to Implementing Offshore Wind Capacities." *Available at SSRN 1137382* (2005).

Leuthold, Florian U., Hannes Weigt, and Christian von Hirschhausen. "A large-scale spatial optimization model of the European electricity market." *Networks and spatial economics* 12, no. 1 (2012): 75-107.

Li, Feng, Dong Yang, Shuaian Wang, and Jinxian Weng. "Ship routing and scheduling problem for steel plants cluster alongside the Yangtze River." *Transportation Research Part E: Logistics and Transportation Review* 122 (2019): 198-210.

Lundmark, Robert, and Linda Warell. "Horizontal mergers in the iron ore industryAn application of PCAIDS." *Resources Policy* 33, no. 3 (2008): 129-141.

Martnez-Zarzoso, Inmaculada, Leandro Garca-Menndez, and Celestino Surez-Burguet. "Impact of transport costs on international trade: the case of Spanish ceramic exports." *Maritime Economics & Logistics* 5, no. 2 (2003): 179-198.

Network, Clarksons Shipping Intelligence. "Dry bulk ship list." (2018)

Neuhoff, Karsten, Carlos Batlle, Gert Brunekreeft, Christos Konstantinidis, Christian Nabe, Giorgia Oggioni, Pablo Rodilla, Sebastian Schwenen, Tomasz Siewierski, and Goran Strbac. "Flexible short-term power trading: Gathering experience in EU countries." (2015).

Notteboom, Theo E. "Complementarity and substitutability among adjacent gateway ports." *Environment and Planning A* 41, no. 3 (2009): 743-762.

Peng, Zixuan, Wenxuan Shan, Feng Guan, and Bin Yu. "Stable vessel-cargo matching in dry bulk shipping market with price game mechanism." *Transportation Research Part E: Logistics and Transportation Review* 95 (2016): 76-94.

Perry, Martin K. "Oligopoly and consistent conjectural variations." *The Bell Journal of Economics* (1982): 197-205.

Pustov, Alexander, Alexander Malanichev, and Ilya Khobotilov. "Long-term iron ore price modeling: Marginal costs vs. incentive price." *Resources Policy* 38, no. 4 (2013): 558-567.

Robson, Edward N., Kasun P. Wijayaratna, and Vinayak V. Dixit. "A review of computable general equilibrium models for transport and their applications in appraisal." *Transportation Research Part A: Policy and Practice* 116 (2018): 31-53.

Shi, Xunpeng, and Hari MP Variam. "East Asias gas-market failure and distinctive economicsA case study of low oil prices." *Applied energy* 195 (2017): 800-809.

Siddiqui, Sauleh, and Steven A. Gabriel. "Modeling market power in the US shale gas market." *Optimization and Engineering* 18, no. 1 (2017): 203-213.

Toweh, Solomon H., and Richard T. Newcomb. "A spatial equilibrium analysis of world iron ore trade." *Resources Policy* 17, no. 3 (1991): 236-248.

Wang, Lafang, Mingyong Lai, and Baojun Zhang. "The transmission effects of iron ore price shocks on China's economy and industries: a CGE approach." *International Journal of Trade and Global Markets* 1, no. 1 (2007): 23-43.

Weigt, Hannes, Karen Freund, and Till Jeske. "Nodal Pricing of the European Electricity Grid-A Welfare Economic Analysis for Feeding-in Offshore Wind Electricity." *Available at SSRN 1137383* (2006).

Wilson, Jeffrey D. "Chinese resource security policies and the restructuring of the Asia-Pacific iron ore market." *Resources Policy* 37, no. 3 (2012): 331-339.

Wing, Ian Sue. "Computable general equilibrium models and their use in economy-wide policy analysis." *Joint Program on the Science and Policy of the Global Change, Technical paper* 6 (2004).

Wogrin, Sonja, Benjamin F. Hobbs, Daniel Ralph, Efraim Centeno, and J. Barqun. "Open versus closed loop capacity equilibria in electricity markets under perfect and oligopolistic competition." *Mathematical Programming* 140, no. 2 (2013): 295-322.

World Steel Association. "World Steel in Figures 2018 Now Available." *World Steel Association: Brussels, Belgium* (2018).

Ye, Qiang. "Commodity booms and their impacts on the Western Australian economy: the iron ore case." *Resources Policy* 33, no. 2 (2008): 83-101.

Zwart, Gijsbert, and Machiel Mulder. *NATGAS: A model of the European natural gas market.* No. 144. CPB Netherlands Bureau for Economic Policy Analysis, 2006.